

pubs.acs.org/JACS Article

Atomic Origin of Chemomechanical Failure of Layered Cathodes in All-Solid-State Batteries

Chunyang Wang, Yaqi Jing, Dong Zhu, and Huolin L. Xin*



ACCESS I Metrics & More Article Recommendations Supporting Information Chunky O1 phase Complex interlayer-shear motifs Surface Frustration TSU NiO nanocrystals Original O3 A-type ,O1-03 Twin-like O3 Failure of layered C-type O1-O3 cathodes in ASSBs

ABSTRACT: The ever-increasing demand for safety has thrust all-solid-state batteries (ASSBs) into the forefront of next-generation energy storage technologies. However, the atomic mechanisms underlying the failure of layered cathodes in ASSBs, as opposed to their counterparts in liquid electrolyte-based lithium-ion batteries (LIBs), have remained elusive. Here, leveraging artificial intelligence-enhanced super-resolution electron microscopy, we unravel the atomic origins dictating the chemomechanical degradation of technologically crucial high-Ni layered oxide cathodes in ASSBs. We reveal that the coupling of surface frustration and interlayer-shear-induced phase transformation exacerbates the chemomechanical breakdown of layered cathodes. Surface frustration, a phenomenon previously unobserved in liquid electrolyte-based LIBs, emerges through electrochemical processes involving surface nanocrystallization coupled with rock salt transformation. Simultaneously, delithiation-induced interlayer shear yields the formation of chunky O1 phases and intricate interfaces/transition motifs, distinct from scenarios observed in liquid electrolyte-based LIBs. Bridging the knowledge gap between the failure mechanisms of layered cathodes in solid-state electrolytes and conventional liquid electrolytes, our study provides unprecedented atomic-scale insights into the degradation pathways of layered cathodes in ASSBs.

INTRODUCTION

All-solid-state batteries (ASSBs) have emerged as one of the most promising next-generation battery technologies, driven by the ever-increasing demand for safer and more efficient energy storage solutions. 1-4 ASSBs, by replacing traditional flammable liquid electrolytes with solid-state electrolytes (SSEs), offer significantly improved safety and thermal stability, which are key to various applications ranging from portable electronics to electric vehicles and grid-scale energy storage. However, despite the considerable progress made in the development of ASSBs, key challenges such as the electrode/electrolyte interfacial instabilities⁵⁻⁸ as well as the underlying failure mechanisms remain to be understood. Among all, one critical issue which limits the performance stability of ASSBs is the electrochemically driven degradation of the layered cathode materials paired with SSEs. In particular, in the pursuit of increasing Ni contents in layered cathodes to achieve higher energy density, 9,10 the intrinsic instability of high-Ni layered oxides 11-14 arising from the ever-increasing Ni content

unavoidably aggravates the chemomechanical failure ^{15–19} of layered cathodes originated from the SSE/cathode interface in ASSBs. As the chemomechanical failure of cathode materials significantly impacts the performance, capacity, and lifespan of ASSBs, understanding the mechanisms driving the degradation of layered cathodes in ASSBs^{20–25} is of paramount importance for the advancement of next-generation battery technology. However, in stark contrast to the extensive research conducted over the last few decades on the degradation of layered cathodes in liquid electrolyte-based lithium-ion batteries (LIBs), ^{26–32} the deep atomic origin underlying the chemo-

Received: February 13, 2024 Revised: June 3, 2024 Accepted: June 4, 2024 Published: June 14, 2024





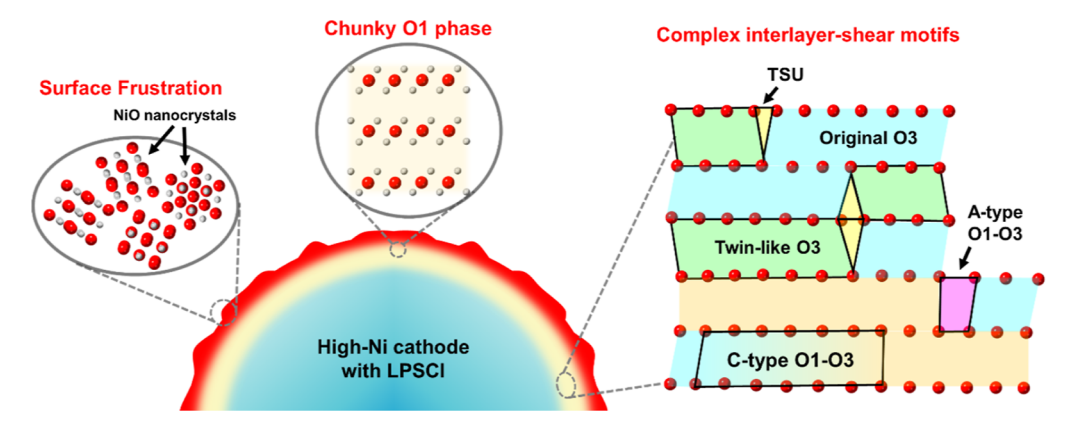


Figure 1. Electrochemically triggered atomic-scale degradation of high-Ni cathodes in ASSBs. The high-Ni cathodes paired with LPSCl degrade through violent surface oxygen loss and nanocrystallization (surface frustration) coupled with subsurface interlayer-shear-induced phase transformation as well as complex interfaces/transition motifs.

mechanical failure of layered cathodes in ASSBs remains a mystery yet to be fully resolved. Unraveling the atomic-scale processes responsible for the degradation will not only deepen our understanding of the fundamental physics involved but also provide crucial insights for the design and development of more robust and durable ASSB systems.

Here, to bridge this gap in knowledge, by combining artificial intelligence (AI)-aided super-resolution imaging and phase segmentation techniques, we first uncovered the atomic origin of the chemomechanical failure mechanism of technologically important high-Ni layered oxide cathodes in sulfide electrolyte-based ASSBs. We reveal that oxygen-lossinduced surface structural frustration and deintercalationinduced interlayer shear collectively destabilize and drive the violent electrochemical breakdown of layered oxides (Figure 1). The surface frustration, which is first identified in layered cathodes, involves the formation of nanosized rock salt polycrystals triggered by severe interfacial oxygen loss. Moreover, new interlayer-shear transition modalities and chunky O1 phases distinct from conventional scenarios in liquid electrolyte-based LIBs are also uncovered. The integration of AI-driven imaging analysis provides unprecedented insights into the intricate processes occurring at the atomic level, shedding light on the degradation pathways and failure mechanisms of layered cathodes in ASSBs. By extending our understanding from liquid electrolyte-based LIBs to solid electrolyte systems, our work addresses a critical knowledge gap in the field of ASSBs, which may pave the way for the development of novel strategies to enhance the durability and performance of layered cathodes in ASSBs.

RESULTS AND DISCUSSION

In this work, a model ASSB is constructed by pairing a model high-Ni layered oxide cathode NMC-811 (see the microstructure of NMC-811 in Figures S1 and S2 with sulfide solid electrolyte LPSCl (see synthesis details in Methods). Figure 2a shows a representative annular dark-field scanning transmission electron microscopy (ADF-STEM) image (taken along the [100] zone axis) of a pristine NMC-811 particle, which exhibits a perfect layered structure (space group: $R\overline{3}m$) with alternate packing of Li layers and transition metal (TM) layers (see an atomic model in the inset). Figure 2b presents the charge—discharge curves of NMC-811/LPSCl ASSBs, showcasing a notable low Coulombic efficiency in the initial cycle followed by rapid capacity decay. Notably, the capacity

retention is approximately 83% after just six cycles, after which the battery ceases to function. Figure 2c presents a representative atomic-resolution ADF-STEM image (see Fourier transforms of different regions in Figure 2d) showing the formation of a chunky O1 phase near the particle surface (the O1/O3 phase boundary is indicated by a dashed line) during delithiation. The ABAB oxygen packing pattern in the O1 phase is clearly identified in the inset of Figure 2c, representing the first experimental evidence of the ABAB oxygen packing in the O1 phase. Figure 2e shows a magnified super-resolution image (obtained by AtomSegNet processing of the ADF-STEM image in Figure 2c) of the large-sized O1 phase formed on the surface of the O3-type layered oxide. In addition, a newly developed AI-aided atom-by-atom phase segmentation technique was also applied to automatically distinguish the O1 phase within the O3 matrix based on the super-resolution images (Figure 2f,g highlights a phase map showing the atomically resolved chunky O1 phase on the particle surface. Note that a slight misorientation [see fast Fourier transform (FFTs) in Figure S3] is identified between the O1 phase and the O3 matrix.

Aside from a large chunk of the O1 phase, solid-state delithiation also leads to the formation of complex O1-O3 mixtures near the particle surface, which consequently results in complex local structures and transition motifs (Figure 3, and see raw images in Figure S4). With the aid of the AI-aided super-resolution technique, the fine atomic structures of the O1-O3 mixtures are precisely resolved and comprehensively analyzed. For example, similar to what is observed in liquid electrolyte-based LIBs, transition motifs such as abrupt/ continuous O1-O3 interfaces (the abrupt and continuous O1-O3 interfaces are indicated by magenta structural units and arrows, respectively) and twin-like domains (TDs, highlighted in green) are also observed in their counterparts in ASSBs (Figure 3a). However, distinct from the scenario in liquid-electrolyte-based LIBs, where only single-layer TDs form, multilayer TDs (e.g., the double-layer TD, as shown in Figure 3b) are also identified for the first time in layered cathodes of ASSBs. The formation of energetically unfavorable multilayer TDs involving consecutive O3 reversal as well as high-density single-layer TDs (see an example in a large-fieldof-view image of a delithiated cathode in Figure 3c) implies that more severe structural damage occurred compared with that in liquid-electrolyte LIBs. Meanwhile, the local nature of the universally formed TDs results in the formation of

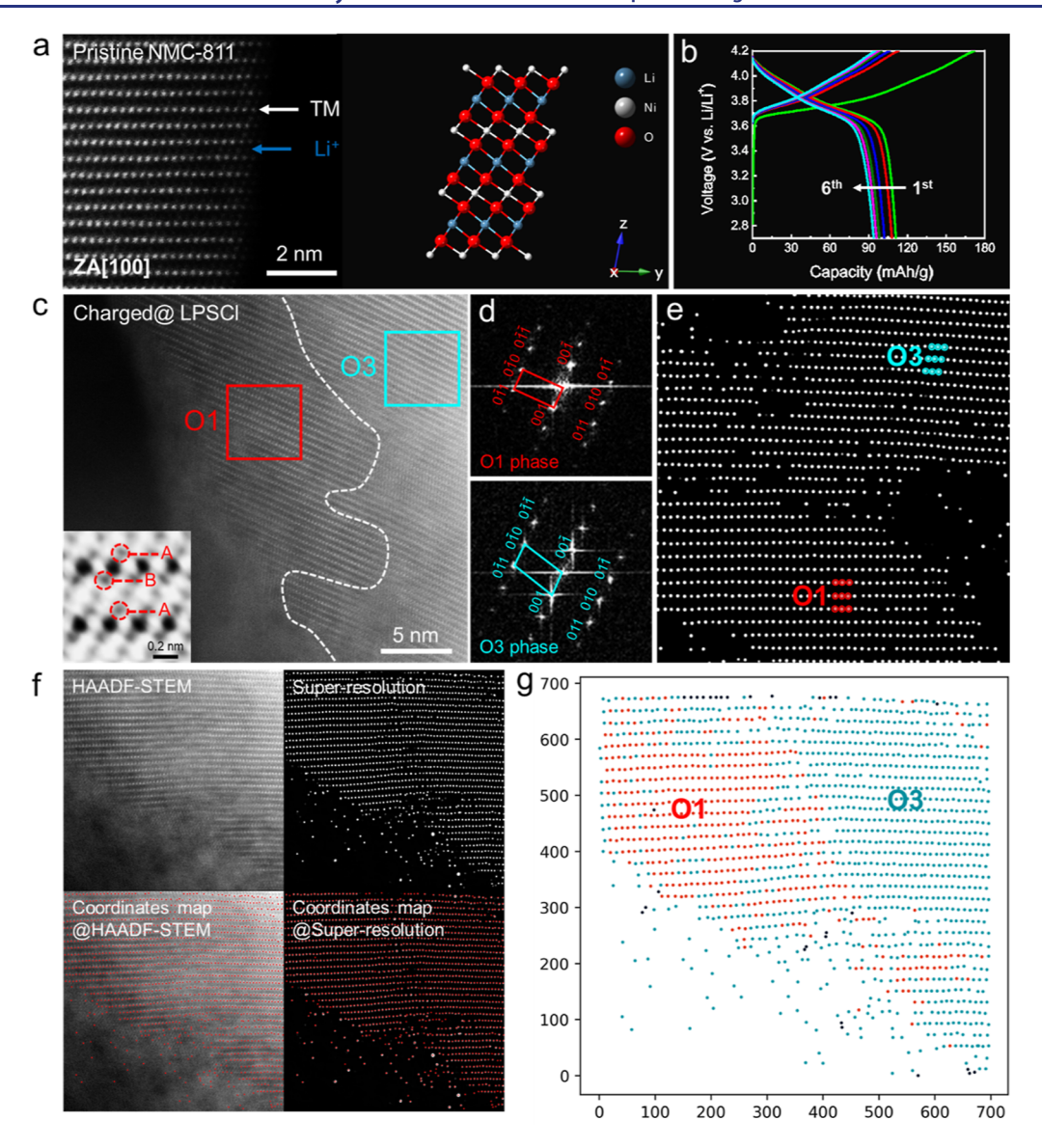


Figure 2. Severe shear phase transformation in delithiated high-Ni cathodes in ASSBs. (a) Atomic-resolution ADF-STEM image and the atomic model of pristine NMC-811, which has a perfect layered structure (space group $R\overline{3}m$). (b) Charge—discharge curves of NMC-811/LPSCl/Li ASSBs operated at 0.1 C rate. The cell died after six cycles. (c) Representative ADF-STEM image of a charged (second cycle, cutoff voltage of 4.2 V) NMC-811 particle taken along the [100] zone axis. Inset shows a representative bright-field (BF)-STEM image of the O1 phase, which has an ABAB oxygen stacking. (d) FFTs corresponding to the boxed regions in (c-e). The super-resolution image highlights a chunky O1 domain adjacent to the O3 matrix in the particle in (c). Note that some atomic columns are not effectively identified due to large sample thickness variation. (f,g) Atomic column localization (left panel) and automated segmentation (right panel) of the O1 phase and the O3 matrix.

constrained twin/matrix interfaces (also termed as O3'/O3 interfaces, where O3' represents a reversed O3 stacking) and, surprisingly, a new structural unit—triangle structural unit (TSU)—is found to form at the O3'/O3 interface in order to accommodate the interfacial misfit.

In addition to the interlayer-shear-induced phase transformation, we also identified severe oxygen loss-triggered surface degradation in delithiated cathodes through both spectroscopic and atomic imaging characterizations. Figure 4a shows representative relatively low-magnification energy-dispersive spectroscopy (EDS) maps of an interface between the LPSCl and NMC-811, where a relatively sharp boundary was identified, while line scan analysis (Figure S5) shows that sulfur (S) and phosphorus (P) are likely involved in the formation of the degraded layers, evidenced by their increased content near the surface, with sulfur being more prominent.

High spatial-resolution electron energy loss spectroscopy (EELS) analysis across the cathode/electrolyte interface shows that the Ni K-edge shifts to lower energy from the interior to the surface of the cathode, indicating an evident reduction of Ni at the electrolyte/cathode interface. Furthermore, atomic-resolution imaging was performed to understand the surface structural degradations triggered by the chemomechanical reaction at the cathode/electrolyte interface. The result shows that a thin layer with a disrupted lattice (approximately 10 nm thick; the boundary between the frustrated layer and the subsurface O1 or O3 phase is denoted by the yellow dashed line) formed on the outer surface of the particle. It is worth noting that the deteriorated crystallinity makes it hard for ADF-STEM to resolve the atomic packing of this structurally frustrated layer; therefore, BF-STEM was further employed to image its atomic structure (the middle of

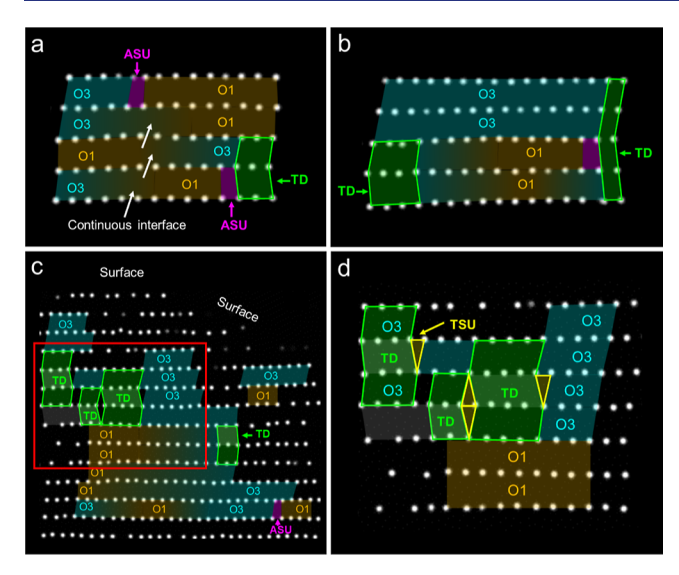


Figure 3. Atomically resolved complex interfaces in delithiated Nirich cathode of ASSBs. (a) Representative super-resolution images showing the formation of abrupt and continuous O1–O3 interfaces as well as twin-like domains (TDs). The abrupt structural units (ASUs) at the O1/O3 and O1/TD interfaces are highlighted in magenta. (b) Super-resolution image of another delithiated particle showing the formation of single-layer (left side) and double-layer (right side) TDs. ASUs are identified at the interface between O1 and TD. (c) Larger field-of-view super-resolution image of a delithiated NMC-811 cathode, which shows the formation of continuous (C-type) and abrupt (A-type) O1–O3 interfaces as well as TDs. (d) Enlarged super-resolution image corresponding to the boxed region in (c). TSUs (yellow symbols) are identified at the interface between the TD (reversed O3) and the original O3 matrix.

Figure 4c). As shown in the right panel of Figure 4c (corresponding to the boxed region in the middle panel), the structurally frustrated layer is found to be composed of ultrasmall nanocrystalline domains (denoted by dashed circles). Based on FFT analysis (inset in the right panel in Figure 4c), the nanocrystals are determined to be composed of electrochemically inactive NiO phases (see another example in Figure S6). This finding indicates that severe oxygen loss was promoted at the cathode/electrolyte interface. That is to say, surface frustration is more likely to develop in primary particles directly interfacing with solid electrolytes, albeit in smaller quantities, than in those situated within the interior of a secondary particle. This may partly explain why surface frustration may not have been previously captured. Conversely, at the chemically contacted cathode/electrolyte interface, we did not observe fragmented rock salt phase or O1 phase (see representative results in Figure S7), indicating that both the concurrent oxygen loss-triggered surface frustration and interlayer-shear-induced phase transformation are chemomechanically driven, rather than chemically driven.

The O1 phase is an interlayer-shear-induced detrimental phase recently found to be extremely vulnerable to oxygen loss and structural degradation. As the tendency of O3 \rightarrow O1 phase transformation increases with increased Ni content, large chunks of the O1 phase have been recently observed in pure LiNiO2 and ultrahigh-Ni cathodes. While, in contrast, for NMC-811, due to its relatively lower Ni content and thereby higher stability (compared to LiNiO2), only random O1 stacking faults (one layer or a few layers thick) have been observed in liquid-electrolyte-based LIBs. 11,33 Surprisingly, we

discovered for the first time that by charging NMC-811 to similar or even lower state-of-charge in ASSBs with LPSCl as the SSE, chunky O1 phase domains, comparable in size to those in pure LiNiO₂, were universally observed. This suggests that the tendency for interlayer shear within the same cathode is significantly intensified by interfacial electrochemical reactions in ASSBs. Note that the absence of the O1 phase in some previous studies^{34,35} may be attributed to the extended cycling conditions employed as this extended cycling regime may have largely depleted the already-formed O1 phase, converting it into the rock salt phase (our previous indicates that the O1 phase is more vulnerable to oxygen loss and cation mixing compared to the O3 phase 16). Moreover, due to the higher tendency of O1 phase transformation, new interfaces and transition motifs, which have never been revealed in the same cathode in liquid electrolyte-based LIBs, were universally revealed. Particularly, the formation of metastable multilayer TDs and O3'/O3 interfaces further confirms the exacerbated chemomechanical degradation of the layered cathode in ASSBs compared to that in conventional liquid-electrolyte-based LIBs.

The surface structural frustration observed in ASSBs differs significantly from the surface rock salt formation seen in conventional liquid-electrolyte-based LIBs. In the case of ternary layered cathodes that exhibit relatively high stability. such as NMC-811, the rock salt transformation typically occurs by forming a coherent rock salt layer (comprising one to a few atomic layers during the early stage of electrochemical cycling) on the particle surface. In previously reported cases in liquid electrolytes, since the transformation from the O3 phase \rightarrow rock salt only requires TM ion diffusion (from the TM layer to the empty sites in the Li layer) without lattice deformation, the electrochemically formed rock salt phase usually shares the same orientation as that of the parental O3 phase,³⁶ meaning the surface rock salt transformation barely breaks the crystallographic integrity of the single-crystalline primary particle. Surprisingly, the surface frustration in ASSBs shows a remarkably different rock salt transformation landscape where nanocrystallization occurs during the electrochemical degradation. The formation of these extremely small nanodomains suggests that chemomechanically triggered local lattice deformation is vigorously involved in the cathode/ electrolyte interfacial degradation from the very beginning. This is markedly different from the scenario in liquid electrolytes, where the chemomechanical factor typically only gradually takes control over extended or long-term cycling. 37,38 Moreover, it is worth noting that the crystallographic integrity broken by surface frustration in ASSBs is expected to be more detrimental in terms of Li⁺ reintercalation. This is because the misorientation between the nanosized rock salt domains creates additional resistance^{39,40} for Li⁺ transportation through the already blocked Li⁺ channels.⁴¹

We propose that interface instabilities, encompassing both electrochemical and mechanical factors between the cathode and the LPSCl solid electrolyte, may play a pivotal role in the formation of a surface frustration layer composed of rock salt nanodomains. From an electrochemical perspective, the degradation mechanisms in ASSBs share similarities with scenarios involving liquid electrolytes, notably involving oxygen loss, cation mixing, and ultimately rock salt formation originating from side reactions at the cathode/electrolyte interface. However, a significant distinction lies in the solid/solid contact in ASSBs, which is inherently rigid. While the sulfide electrolyte is softer than other inorganic electrolytes, it

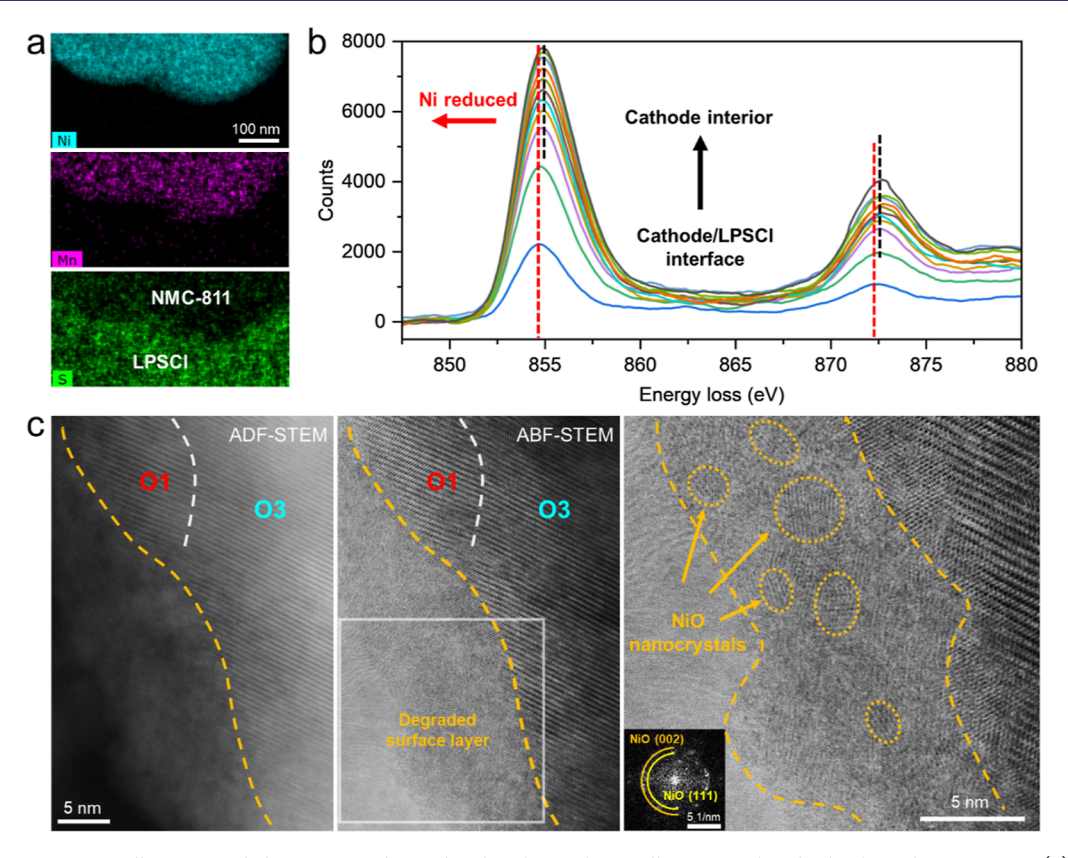


Figure 4. Surface nanocrystallization and deactivation driven by the electrochemically triggered cathode-electrolyte reaction. (a) EDS maps of pristine NMC-811 cathode particles in contact with LPSCl after electrochemical cycling. (b) EELS profiles of charged (second cycle) NMC-811 from the cathode–electrolyte interface to the cathode particle's interior. The evidently reduced Ni valence near the cathode's surface indicates severe oxygen loss at the cathode–electrolyte interface. (c) Representative ADF-STEM (left panel) and BF-STEM (middle panel) images showing the electrochemically driven oxygen loss and structural degradation at the cathode surface. The right panel shows a zoomed-in image corresponding to the boxed region in the middle panel. The atomic structure of the nanodomains (highlighted by dashed circles) can be assigned to the rock salt phase, which also agrees well with the FFT of the degraded surface layer (inset).

is still significantly stiffer than liquid electrolytes. Consequently, unlike scenarios with liquid electrolytes, the rigidity of SSEs in ASSBs may contribute to localized stress accumulation within the cathode material. This local stress could even be exacerbated under externally applied pressure during ASSB fabrication processes aimed at enhancing interface contact. We suspect that this local stress concentration may promote chemomechanical disintegration of the as-formed rock salt phase to form nanodomains with different orientations. Simultaneously, it could also promote interlayer shear in the near-surface regions, ultimately resulting in O1 phase transformation. In the future, in situ TEM techniques might be employed to further understand the formation pathway of the unique chemomechanical degradation structures of layered cathodes in ASSBs.

By delving into the atomic-scale mechanisms governing the failure of layered cathodes in ASSBs, we can envisage several strategies that could potentially mitigate chemomechanical degradation and enhance ASSB performance. First, surface engineering offers the possibility of designing cathode materials that are more resistant to surface nanocrystallization and rock salt transformation during electrochemical processes. Surface coating 42 emerges as a potential solution to mitigate the adverse effects of surface frustration observed in our study, potentially leading to a more stable cathode/electrolyte interface. Second, the concept of bulk lattice reinforcement suggests that designing a stronger bulk lattice with antishear

properties could be beneficial. Leveraging bulk doping, including the recently proposed compositionally complex doping strategy, may enhance the mechanical resilience of cathode particles and potentially mitigate interlayer shear-induced degradation. This work underscores the critical importance of safeguarding both the surface (or, the cathode/electrolyte interface) and the bulk lattice of layered oxide cathodes in ASSBs.

CONCLUSIONS

In conclusion, using AI-aided super-resolution atomic imaging, we uncovered that the coupling of surface frustration and shear transformation leads to extended chemomechanical degradation of technologically important high-Ni layered cathodes in ASSBs. The electrochemically induced degradation, which involves misoriented nanoscale rock salt transformation and complex shear structural motifs, represents a phenomenon distinctively different from that observed in liquid-electrolytebased LIB cathodes. These new insights provide a profound understanding of the degradation pathway of layered oxides in ASSBs and underscore the pivotal role of enhancing the electrochemical stability of cathode—electrolyte interfaces in optimizing current ASSBs.

ASSOCIATED CONTENT

3 Supporting Information

The Supporting Information is available free of charge at https://pubs.acs.org/doi/10.1021/jacs.4c02198.

Materials and electrochemical tests; details of TEM experiments; and additional SEM, TEM, and atomic-resolution STEM images of pristine and layered oxide cathode after cycling (PDF)

AUTHOR INFORMATION

Corresponding Author

Huolin L. Xin — Department of Physics and Astronomy, University of California Irvine, Irvine, California 92697, United States; ⊚ orcid.org/0000-0002-6521-868X; Email: huolin.xin@uci.edu

Authors

Chunyang Wang — Department of Physics and Astronomy, University of California Irvine, Irvine, California 92697, United States; Shenyang National Laboratory for Materials Science, Institute of Metal Research, Chinese Academy of Sciences, Shenyang 110016, China; orcid.org/0000-0001-8461-3952

Yaqi Jing — Department of Physics and Astronomy, University of California Irvine, Irvine, California 92697, United States Dong Zhu — Department of Physics and Astronomy, University of California Irvine, Irvine, California 92697, United States; orcid.org/0009-0008-5314-1452

Complete contact information is available at: https://pubs.acs.org/10.1021/jacs.4c02198

Notes

The authors declare no competing financial interest.

ACKNOWLEDGMENTS

This work is supported by the Office of Basic Energy Sciences of the U.S. Department of Energy, under award no. DE-SC0021204. We acknowledge the use of facilities and instrumentation at the UC Irvine Materials Research Institute, which is supported in part by the National Science Foundation through the UC Irvine Materials Research Science and Engineering Center (no. DMR-2011967). Part of the writeup was completed after C.Y.W. departed from UC Irvine.

REFERENCES

- (1) Janek, J.; Zeier, W. G. Challenges in speeding up solid-state battery development. *Nat. Energy* **2023**, *8* (3), 230–240.
- (2) Randau, S.; Weber, D. A.; Kötz, O.; Koerver, R.; Braun, P.; Weber, A.; Ivers-Tiffée, E.; Adermann, T.; Kulisch, J.; Zeier, W. G.; Richter, F. H.; Janek, J. Benchmarking the performance of all-solid-state lithium batteries. *Nat. Energy* **2020**, *5* (3), 259–270.
- (3) Hao, F.; Han, F.; Liang, Y.; Wang, C.; Yao, Y. Architectural design and fabrication approaches for solid-state batteries. *MRS Bull.* **2018**, 43 (10), 775–781.
- (4) Deng, S.; Li, X.; Ren, Z.; Li, W.; Luo, J.; Liang, J.; Liang, J.; Banis, M. N.; Li, M.; Zhao, Y.; Li, X.; Wang, C.; Sun, Y.; Sun, Q.; Li, R.; Hu, Y.; Huang, H.; Zhang, L.; Lu, S.; Luo, J.; Sun, X. Dual-functional interfaces for highly stable Ni-rich layered cathodes in sulfide all-solid-state batteries. *Energy Storage Mater.* **2020**, *27*, 117–123
- (5) Xiao, Y.; Wang, Y.; Bo, S.-H.; Kim, J. C.; Miara, L. J.; Ceder, G. Understanding interface stability in solid-state batteries. *Nat. Rev. Mater.* **2019**, 5 (2), 105–126.

- (6) Chen, R.; Li, Q.; Yu, X.; Chen, L.; Li, H. Approaching Practically Accessible Solid-State Batteries: Stability Issues Related to Solid Electrolytes and Interfaces. *Chem. Rev.* **2020**, *120* (14), 6820–6877.
- (7) Liang, Z.; Xiao, Y.; Wang, K.; Jin, Y.; Pan, S.; Zhang, J.; Wu, Y.; Su, Y.; Zhong, H.; Yang, Y. Enabling stable and high areal capacity solid state battery with Ni-rich cathode via failure mechanism study. *Energy Storage Mater.* **2023**, *63*, 102987.
- (8) Ai, Q.; Chen, Z.; Zhang, B.; Wang, F.; Zhai, T.; Liu, Y.; Zhu, Y.; Terlier, T.; Fang, Q.; Liang, Y.; Zhao, L.; Wu, C.; Guo, H.; Fan, Z.; Tang, M.; Yao, Y.; Lou, J. High-Spatial-Resolution Quantitative Chemomechanical Mapping of Organic Composite Cathodes for Sulfide-Based Solid-State Batteries. *ACS Energy Lett.* **2023**, 8 (2), 1107–1113.
- (9) Zhang, R.; Wang, C.; Zou, P.; Lin, R.; Ma, L.; Yin, L.; Li, T.; Xu, W.; Jia, H.; Li, Q.; Sainio, S.; Kisslinger, K.; Trask, S. E.; Ehrlich, S. N.; Yang, Y.; Kiss, A. M.; Ge, M.; Polzin, B. J.; Lee, S. J.; Xu, W.; Ren, Y.; Xin, H. L. Compositionally complex doping for zero-strain zero-cobalt layered cathodes. *Nature* **2022**, *610*, 67–73.
- (10) Wang, L.; Mukherjee, A.; Kuo, C. Y.; Chakrabarty, S.; Yemini, R.; Dameron, A. A.; DuMont, J. W.; Akella, S. H.; Saha, A.; Taragin, S.; Aviv, H.; Naveh, D.; Sharon, D.; Chan, T. S.; Lin, H. J.; Lee, J. F.; Chen, C. T.; Liu, B.; Gao, X.; Basu, S.; Hu, Z.; Aurbach, D.; Bruce, P. G.; Noked, M. High-energy all-solid-state lithium batteries enabled by Co-free LiNiO(2) cathodes with robust outside-in structures. *Nat. Nanotechnol.* 2024, *19*, 208–218.
- (11) Wang, C.; Wang, X.; Zhang, R.; Lei, T.; Kisslinger, K.; Xin, H. L. Resolving complex intralayer transition motifs in high-Ni-content layered cathode materials for lithium-ion batteries. *Nat. Mater.* **2023**, 22 (2), 235–241.
- (12) Cheng, J.; Ouyang, B.; Persson, K. A. Mitigating the High-Charge Detrimental Phase Transformation in LiNiO2 Using Doping Engineering. ACS Energy Lett. 2023, 8 (5), 2401–2407.
- (13) Zhang, R.; Wang, C.; Zou, P.; Lin, R.; Ma, L.; Li, T.; Hwang, I.h.; Xu, W.; Sun, C.; Trask, S.; Xin, H. L. Long-life lithium-ion batteries realized by low-Ni, Co-free cathode chemistry. *Nat. Energy* **2023**, *8*, 695–702.
- (14) Meng, X. H.; Lin, T.; Mao, H.; Shi, J. L.; Sheng, H.; Zou, Y. G.; Fan, M.; Jiang, K.; Xiao, R. J.; Xiao, D.; Gu, L.; Wan, L. J.; Guo, Y. G. Kinetic Origin of Planar Gliding in Single-Crystalline Ni-Rich Cathodes. J. Am. Chem. Soc. 2022, 144 (25), 11338–11347.
- (15) Wang, C.; Wang, X.; Zou, P.; Zhang, R.; Wang, S.; Song, B.; Low, K.-B.; Xin, H. L. Direct observation of chemomechanical stress-induced phase transformation in high-Ni layered cathodes for lithium-ion batteries. *Matter* **2023**, *6* (4), 1265–1277.
- (16) Wang, C.; Han, L.; Zhang, R.; Cheng, H.; Mu, L.; Kisslinger, K.; Zou, P.; Ren, Y.; Cao, P.; Lin, F.; Xin, H. L. Resolving atomic-scale phase transformation and oxygen loss mechanism in ultrahigh-nickel layered cathodes for cobalt-free lithium-ion batteries. *Matter* **2021**, *4* (6), 2013–2026.
- (17) Bi, Y.; Tao, J.; Wu, Y.; Li, L.; Xu, Y.; Hu, E.; Wu, B.; Hu, J.; Wang, C.; Zhang, J.-G.; Qi, Y.; Xiao, J. Reversible planar gliding and microcracking in a single-crystalline Ni-rich cathode. *Science* **2020**, 370 (6522), 1313–1317.
- (18) Li, J.; Sharma, N.; Jiang, Z.; Yang, Y.; Monaco, F.; Xu, Z.; Hou, D.; Ratner, D.; Pianetta, P.; Cloetens, P.; Lin, F.; Zhao, K.; Liu, Y. Dynamics of particle network in composite battery cathodes. *Science* **2022**, *376* (6592), 517–521.
- (19) Zou, Y. G.; Mao, H.; Meng, X. H.; Du, Y. H.; Sheng, H.; Yu, X.; Shi, J. L.; Guo, Y. G. Mitigating the Kinetic Hindrance of Single-Crystalline Ni-Rich Cathode via Surface Gradient Penetration of Tantalum. *Angew. Chem., Int. Ed.* **2021**, *60* (51), 26535–26539.
- (20) Deng, S.; Sun, Q.; Li, M.; Adair, K.; Yu, C.; Li, J.; Li, W.; Fu, J.; Li, X.; Li, R.; Hu, Y.; Chen, N.; Huang, H.; Zhang, L.; Zhao, S.; Lu, S.; Sun, X. Insight into cathode surface to boost the performance of solid-state batteries. *Energy Storage Mater.* **2021**, *35*, *661–668*.
- (21) Liang, J.; Zhu, Y.; Li, X.; Luo, J.; Deng, S.; Zhao, Y.; Sun, Y.; Wu, D.; Hu, Y.; Li, W.; Sham, T. K.; Li, R.; Gu, M.; Sun, X. A gradient oxy-thiophosphate-coated Ni-rich layered oxide cathode for stable all-solid-state Li-ion batteries. *Nat. Commun.* **2023**, *14* (1), 146.

- (22) Wang, J.; Zhang, Z.; Han, J.; Wang, X.; Chen, L.; Li, H.; Wu, F. Interfacial and cycle stability of sulfide all-solid-state batteries with Nirich layered oxide cathodes. *Nano Energy* **2022**, *100*, 107528.
- (23) Zhang, J.; Zheng, C.; Li, L.; Xia, Y.; Huang, H.; Gan, Y.; Liang, C.; He, X.; Tao, X.; Zhang, W. Unraveling the Intra and Intercycle Interfacial Evolution of Li6PSSCl-Based All-Solid-State Lithium Batteries. *Adv. Energy Mater.* **2019**, *10* (4), 1903311.
- (24) Liang, Z.; Xiang, Y.; Wang, K.; Zhu, J.; Jin, Y.; Wang, H.; Zheng, B.; Chen, Z.; Tao, M.; Liu, X.; Wu, Y.; Fu, R.; Wang, C.; Winter, M.; Yang, Y. Understanding the failure process of sulfide-based all-solid-state lithium batteries via operando nuclear magnetic resonance spectroscopy. *Nat. Commun.* 2023, 14 (1), 259.
- (25) Wu, C.; Lou, J.; Zhang, J.; Chen, Z.; Kakar, A.; Emley, B.; Ai, Q.; Guo, H.; Liang, Y.; Lou, J.; Yao, Y.; Fan, Z. Current status and future directions of all-solid-state batteries with lithium metal anodes, sulfide electrolytes, and layered transition metal oxide cathodes. *Nano Energy* **2021**, *87*, 106081.
- (26) Liu, T.; Liu, J.; Li, L.; Yu, L.; Diao, J.; Zhou, T.; Li, S.; Dai, A.; Zhao, W.; Xu, S.; Ren, Y.; Wang, L.; Wu, T.; Qi, R.; Xiao, Y.; Zheng, J.; Cha, W.; Harder, R.; Robinson, I.; Wen, J.; Lu, J.; Pan, F.; Amine, K. Origin of structural degradation in Li-rich layered oxide cathode. *Nature* 2022, 606 (7913), 305–312.
- (27) Yan, P.; Zheng, J.; Tang, Z. K.; Devaraj, A.; Chen, G.; Amine, K.; Zhang, J. G.; Liu, L. M.; Wang, C. Injection of oxygen vacancies in the bulk lattice of layered cathodes. *Nat. Nanotechnol.* **2019**, *14* (6), 602–608
- (28) Liu, T.; Yu, L.; Liu, J.; Lu, J.; Bi, X.; Dai, A.; Li, M.; Li, M.; Hu, Z.; Ma, L.; Luo, D.; Zheng, J.; Wu, T.; Ren, Y.; Wen, J.; Pan, F.; Amine, K. Understanding Co roles towards developing Co-free Nirich cathodes for rechargeable batteries. *Nat. Energy* **2021**, *6* (3), 277–286.
- (29) Li, H.; Wang, L.; Song, Y.; Wu, Y.; Zhang, H.; Du, A.; He, X. Understanding the Insight Mechanism of Chemical-Mechanical Degradation of Layered Co-Free Ni-Rich Cathode Materials: A Review. *Small* **2023**, *19* (32), 2302208.
- (30) Zhou, T.; Wang, H.; Wang, Y.; Jiao, P.; Hao, Z.; Zhang, K.; Xu, J.; Liu, J.-B.; He, Y.-S.; Zhang, Y.-X.; Chen, L.; Li, L.; Zhang, W.; Ma, Z.-F.; Chen, J. Stabilizing lattice oxygen in slightly Li-enriched nickel oxide cathodes toward high-energy batteries. *Chem* **2022**, 8 (10), 2817–2830.
- (31) Wang, C.; Zhang, R.; Siu, C.; Ge, M.; Kisslinger, K.; Shin, Y.; Xin, H. L. Chemomechanically Stable Ultrahigh-Ni Single-Crystalline Cathodes with Improved Oxygen Retention and Delayed Phase Degradations. *Nano Lett.* **2021**, 21 (22), 9797–9804.
- (32) Wang, C.; Zhang, R.; Kisslinger, K.; Xin, H. L. Atomic-Scale Observation of O1 Faulted Phase-Induced Deactivation of LiNiO2 at High Voltage. *Nano Lett.* **2021**, *21* (8), 3657–3663.
- (33) Zhu, D.; Wang, C.; Zou, P.; Zhang, R.; Wang, S.; Song, B.; Yang, X.; Low, K. B.; Xin, H. L. Deep-Learning Aided Atomic-Scale Phase Segmentation toward Diagnosing Complex Oxide Cathodes for Lithium-Ion Batteries. *Nano Lett.* **2023**, *23* (17), 8272–8279.
- (34) Wang, Z.; Wang, Z.; Xue, D.; Zhao, J.; Zhang, X.; Geng, L.; Li, Y.; Du, C.; Yao, J.; Liu, X.; Rong, Z.; Guo, B.; Fang, R.; Su, Y.; Delmas, C.; Harris, S. J.; Wagemaker, M.; Zhang, L.; Tang, Y.; Zhang, S.; Zhu, L.; Huang, J. Reviving the rock-salt phases in Ni-rich layered cathodes by mechano-electrochemistry in all-solid-state batteries. *Nano Energy* 2023, 105, 108016.
- (35) Zhang, X.; Wang, Z.; Li, X.; Su, Y.; Ye, Z.; Zhang, L.; Huang, Q.; Tang, Y.; Huang, J. Assessing the roles of mechanical cracks in Nirich layered cathodes in the capacity decay of liquid and solid-state batteries. *Mater. Horiz.* **2023**, *10* (5), 1856–1864.
- (36) Lin, F.; Markus, I. M.; Nordlund, D.; Weng, T. C.; Asta, M. D.; Xin, H. L.; Doeff, M. M. Surface reconstruction and chemical evolution of stoichiometric layered cathode materials for lithium-ion batteries. *Nat. Commun.* **2014**, *5* (1), 3529.
- (37) Yan, P.; Zheng, J.; Gu, M.; Xiao, J.; Zhang, J.-G.; Wang, C.-M. Intragranular cracking as a critical barrier for high-voltage usage of layer-structured cathode for lithium-ion batteries. *Nat. Commun.* **2017**, *8* (1), 14101.

- (38) Yan, P.; Zheng, J.; Chen, T.; Luo, L.; Jiang, Y.; Wang, K.; Sui, M.; Zhang, J. G.; Zhang, S.; Wang, C. Coupling of electrochemically triggered thermal and mechanical effects to aggravate failure in a layered cathode. *Nat. Commun.* **2018**, 9 (1), 2437.
- (39) Ahmed, S.; Volz, K. Stressed during cycling: Electrochemically induced mechanical deformation in Ni-rich cathode materials. *Matter* **2023**, *6* (6), 1682–1684.
- (40) Lee, S. Y.; Park, G. S.; Jung, C.; Ko, D. S.; Park, S. Y.; Kim, H. G.; Hong, S. H.; Zhu, Y.; Kim, M. Revisiting Primary Particles in Layered Lithium Transition-Metal Oxides and Their Impact on Structural Degradation. *Adv. Sci.* **2019**, *6* (6), 1800843.
- (41) Ahmed, S.; Pokle, A.; Bianchini, M.; Schweidler, S.; Beyer, A.; Brezesinski, T.; Janek, J.; Volz, K. Understanding the formation of antiphase boundaries in layered oxide cathode materials and their evolution upon electrochemical cycling. *Matter* **2021**, *4* (12), 3953–3966.
- (42) Zhao, C.; Wang, C.; Liu, X.; Hwang, I.; Li, T.; Zhou, X.; Diao, J.; Deng, J.; Qin, Y.; Yang, Z.; Wang, G.; Xu, W.; Sun, C.; Wu, L.; Cha, W.; Robinson, I.; Harder, R.; Jiang, Y.; Bicer, T.; Li, J.-T.; Lu, W.; Li, L.; Liu, Y.; Sun, S.-G.; Xu, G.-L.; Amine, K. Suppressing strain propagation in ultrahigh-Ni cathodes during fast charging via epitaxial entropy-assisted coating. *Nat. Energy* **2024**, *9*, 345–356.